Available online at www.sciencedirect.com
SCIENCE DIRECT®
Journal of Computational Physics 189 (2003) 111–129
JOURNAL OF COMPUTATIONAL PHYSICS
www.elsevier.com/locate/jcp

Investigation of a two-dimensional spectral element method for Helmholtz's equation

Omid Z. Mehdizadeh [a], Marius Paraschivoiu [b,*]

[a] *Department of Mechanical and Industrial Engineering, University of Toronto, Ont., Canada M5S 3G8*
[b] *Department of Mechanical and Industrial Engineering, Concordia University, Room H549, 1455 de Maisonneuve Blvd. West, Montreal, Que., Canada H3G 1M8*

Received 16 May 2002; received in revised form 14 March 2003; accepted 20 March 2003

Abstract

A spectral element method is developed for solving the two-dimensional Helmholtz's equation, which is the equation governing time-harmonic acoustic waves. Computational cost for solving Helmholtz's equation with the Galerkin finite element method increases as the wave number increases, due to the pollution effect. Therefore a more efficient numerical method is sought. The comparison between a spectral element method and a second-order finite element method shows that the spectral element method leads to fewer grid points per wavelength and less computational cost, for the same accuracy. It also offers the same advantage as the finite element method to address complex geometry and general material property. Some simple examples are addressed and compared with the exact solutions to confirm the accuracy of the method. For unbounded problems, the symmetric perfectly matched layer (PML) method is applied to treat the non-reflecting boundary conditions. In the PML method, a fictitious absorbing layer is introduced outside the truncated boundary.

1. Introduction

Time-harmonic wave propagation, either elastic waves or electromagnetic waves, is a common phenomenon that appears in many applications such as acoustic wave scattering from submarines [1], noise reduction in silencers and mufflers [2], earthquake wave propagation [3], light distribution in radiative optical fiber devices [4], fluid–structure interaction [5], sea-wave propagation [6] and radar scattering [7]. The time-harmonic wave propagation is governed by Helmholtz's equation. In other words, boundary value problems governed by Helmholtz's equation are abundant in many branches of science and technology such as acoustics, seismology, optics, geophysics, electrodynamics and fluid dynamics.

Different numerical approaches have been developed to address boundary value problems governed by Helmholtz's equation. For many years the classic approach to solve this equation has been based on boundary

* Corresponding author.
E-mail addresses: omidzm@mie.utoronto.ca (O.Z. Mehdizadeh), paraschi@me.concordia.ca (M. Paraschivoiu).

0021-9991/03/$ - see front matter
doi:10.1016/S0021-9991(03)00204-3

element method [8]. These methods are based on integration over the boundary of the problem and can naturally address unbounded problems. The disadvantages of boundary element methods are the restriction to linear problems in homogeneous and isotropic media, and their difficulty with characteristic wave numbers in the interior problems [9]. Furthermore, from the numerical point of view, boundary element methods lead to ill-conditioned systems, which are expensive to solve, especially for three-dimensional problems.

Finite element methods have recently become more popular to solve the Helmholtz's equation [10]. These methods do not have the restrictions of boundary element methods, but need special treatment for unbounded problems [11]. These methods lead to sparse matrices, which can be solved iteratively. The cost comparison of finite element and boundary element methods shows that finite element methods are comparable with boundary element methods for solution of acoustic scattering problems [12].

A significant weakness of the Galerkin finite element method for solving Helmholtz's equation is the so-called pollution effect [13]. This terminology indicates that for higher wave numbers more nodes per wavelength are needed than for lower wave numbers to achieve the same solution accuracy.

In order to improve the efficiency of the classical Galerkin approximation, some modifications have been developed [14]. These modifications aim to minimize the pollution effect caused by spurious dispersion of the numerical computation [15]. The most common approach is the Galerkin/least-squares (GLS) method, which is based on appending residuals of the Euler–Lagrange equations in the least squares form to the standard Galerkin formulation [16]. Those additional terms are constant dependent. Finding the optimal GLS constants is a challenge [17].

In this work, a two-dimensional spectral element methods is investigated as an alternative to finite element methods. The spectral element method has polynomial basis functions of degree N in each spatial dimension, and integrals over the elements are evaluated using numerical quadrature [18]. Spectral element methods have been shown to be efficient for elliptic problems in other applications such as fluid mechanics [19]. For Helmholtz's problems, it is shown herein that it requires fewer grid points per wavelength compared to finite element methods. This translates into smaller systems to solve for the same accuracy. Although the resulting smaller matrix is less sparse compare to the resulting finite element matrix, it requires less computational time to be solved iteratively, provided that an appropriate preconditioner is applied. High wave numbers are investigated in this work to demonstrate the range of applications of the spectral element method.

As mentioned before, a special treatment is needed to address unbounded problems when using finite element methods. This work does not focus on the different approaches for solving unbounded problems, but demonstrates that methods that worked well for finite element methods also work for spectral element methods. A recently developed approach, which is called perfectly matched layer (PML), is applied here [20]. It is based on introducing an absorptive layer outside the truncated boundary to damp all the waves entering it.

The reminder of this paper is organized as follows. Section 2 introduces the model problems investigated herein. Section 3 is devoted to details of the numerical approximation. The spectral element discretization, numerical quadrature and assembly of the resulting matrix are discussed in this section. In Section 4, the numerical results for three sample problems are reported. The investigation of the efficiency of the method for sample problems is discussed in Section 5. Finally a conclusion is given in Section 6.

2. Model problems

2.1. Governing equation

Linear wave propagation in a medium is described by the wave equation

$$\frac{1}{c^2}\frac{\partial^2\phi(x,y,t)}{\partial t^2} - \nabla^2\phi(x,y,t) = F(x,y,t), \tag{1}$$

where ϕ is the velocity potential, c is the wave propagation speed and F is a source function. The velocity and pressure in the medium of interest are derived from the velocity potential by the following two relations:

$$u(x,y,t) = -\nabla\phi(x,y,t), \tag{2}$$

$$p(x,y,t) = \rho\frac{\partial\phi(x,y,t)}{\partial t}. \tag{3}$$

By assuming a time-harmonic solution for the velocity potential, $\phi(x,y,t) = \varphi(x,y)e^{i\omega t}$, and a time-harmonic source function $F(x,y,t) = f(x,y)e^{i\omega t}$, the wave Eq. (1) reduces to Helmholtz's equation

$$\nabla^2\varphi(x,y) + k^2\varphi(x,y) = -f(x,y), \tag{4}$$

where k is the wave number defined as

$$k = \frac{\omega}{c}, \tag{5}$$

and ω is the angular velocity.

Clearly the solution of (4) requires boundary conditions. Three different boundary conditions are investigated in Section 2.2. As in finite element methods, spectral element methods solve the variational form of Helmholtz's equation.

Let Ω be an infinite domain exterior to a closed surface Γ or an interior domain bounded by Γ. Given $Z = \{v = v_R + iv_I : v_R \in H^1(\Omega), v_I \in H^1(\Omega)\}$, the variational formulation of this problem with homogeneous boundary conditions is: find $\varphi \in Z$ such that

$$a(\varphi, v) = (f, v) \quad \forall v \in Z, \tag{6}$$

where the bilinear and linear forms are defined as

$$a(\varphi, v) \equiv \int_\Omega (\nabla\varphi\cdot\nabla v - k^2\varphi v)\mathrm{d}x\,\mathrm{d}y, \tag{7}$$

$$(f, v) \equiv \int_\Omega fv\mathrm{d}x\,\mathrm{d}y. \tag{8}$$

2.2. Boundary conditions

Two boundary conditions are common in acoustics. Dirichlet boundary conditions $\varphi = \varphi_0$ are associated with known pressure amplitude on a boundary, which occurs on vibrating boundaries. Homogeneous Neumann boundary conditions $\partial\varphi/\partial n = 0$ (n is the unit vector normal to the boundary surface) are associated with zero velocity on a boundary, which occurs on rigid walls. These two boundary conditions are straightforward to implement, and do not need additional explanations.

Problems on unbounded domains, appearing in many applications, require special boundary conditions. For domain-based numerical methods, such as spectral element methods, it is obviously impractical to solve the problem on the unbounded domain. An artificial boundary is usually introduced by truncating the unbounded domain. This artificial boundary must be designed in such a way that it does not introduce reflecting waves, which do not exist in the original unbounded problem. The appropriate radiation condition, Sommerfeld radiation condition, must be satisfied:

$$\lim_{|r|\to\infty} |r|^{(d-1)/2}\left(\frac{\partial\varphi}{\partial n} - ik\varphi\right) = 0, \tag{9}$$

where d is the spatial dimension and r is the radial direction.

A classic approach to non-reflecting boundary conditions is the DtN (Dirichlet to Neumann) method. In this method the artificial boundary is selected to be of a simple geometric shape, such as a circle in two dimensions. This simple geometric shape allows an analytical solution to the problem in the exterior domain with arbitrary Dirichlet conditions on the artificial boundary. Problems in the interior domain are then solved numerically, coupled with the analytical solution of the exterior domain. The DtN method is hard to implement because of constraints on the shape of the artificial boundary and uniqueness concerns of the external solution.

The method chosen here to create a non-reflecting boundary condition on the artificial boundary is called PML. This method has gained popularity recently, because it does not have the restrictions of the DtN method and it is easy to implement. The PML method is based on introducing an absorbing layer, after the truncated boundary, to absorb outgoing waves and prevent reflection from the artificial boundary. Based on this method the variational form of Eq. (6) is changed to

$$\int_{\Omega} (\nabla v \cdot D \nabla \varphi - v K_x K_y \varphi) \mathrm{d}\Omega = (f, v) \quad \forall v \in H^1, \tag{10}$$

where

$$D = \begin{bmatrix} \frac{K_y}{K_x} & 0 \\ 0 & \frac{K_x}{K_y} \end{bmatrix}, \tag{11}$$

and

$$\begin{aligned} K_x &= k - \mathrm{i}\sigma_x(x), \\ K_y &= k - \mathrm{i}\sigma_y(y). \end{aligned} \tag{12}$$

Eq. (10) reduces to the original Eq. (6) when the coefficients $\sigma_x(x)$ and $\sigma_y(y)$ are zero, which is true in the physical domain. The coefficients are defined to vary from zero at the interface (for the "perfect match") to a maximum value at the truncation of the layer. In layers on the right and left of the main domain $\sigma_y(y)$ is zero and similarly, for top and bottom layers, $\sigma_x(x)$ is zero. In corner absorbing layer regions, both $\sigma_x(x)$ and $\sigma_y(y)$ have non-zero values.

3. The spectral element method

3.1. Spectral element discretization

The spectral element method used herein divides the computational domain Ω into K disjoint rectangular elements, Ω_k, $k = 1, \ldots K$, such that

$$\bar{\Omega} = \bigcup_{k=1}^{K} \bar{\Omega}_k. \tag{13}$$

The discrete space is defined as

$$Z_N = \{v = v_{\mathrm{R}} + \mathrm{i}v_{\mathrm{I}} : v_{\mathrm{R}}|_{\Omega_k} \in Q_N(\Omega_k), v_{\mathrm{I}}|_{\Omega_k} \in Q_N(\Omega_k),\ k = 1, \ldots, K\} \cap Z, \tag{14}$$

where Q_N denotes the space of polynomials of degree $\leqslant N$ in each spatial direction. Therefore, in each element, the solution is approximated with Legendre based polynomials of order N in each spatial

direction. A reference element $\hat{\Omega} = (-1,1)^2$ is introduced in practice to simplify the spectral element implementation.

A nodal basis for the reference element is built by Lagrangian basis polynomials associated with a tensor product grid of Gauss–Labatto–Legendre (GLL) nodes. An example of such a grid is shown in Fig. 1 for a nineth-order polynomial space. The GLL grid nodes in one direction, $\bar{\xi}_j \in [-1,1]$, $0 \leqslant j \leqslant N$ are the roots of the polynomial

$$\left(1-x^2\right)\frac{\mathrm{d}P_N(x)}{\mathrm{d}x}, \tag{15}$$

where $P_N(x)$ is the Legendre polynomial of degree N in $[-1,1]$:

$$\begin{aligned} &P_0(x) = 1, \\ &P_1(x) = x, \\ &P_{n+1}(x) = \frac{2n+1}{n+1}xP_{n+1}(x) - \frac{n}{n+1}P_{n-1}(x), \quad n \geqslant 1. \end{aligned} \tag{16}$$

The basis functions are constructed as a set of Lagrange interpolants. The Lagrange interpolant associated with the ith and jth grid node is defined as

$$h_{ij}(\xi_1,\xi_2) = \prod_{\substack{m=0 \\ m\neq i}}^{\mathrm{N}} \frac{(\xi_1-\bar{\xi}_m)}{(\bar{\xi}_i-\bar{\xi}_m)} \prod_{\substack{n=0 \\ n\neq j}}^{\mathrm{N}} \frac{(\xi_2-\bar{\xi}_n)}{(\bar{\xi}_j-\bar{\xi}_n)}, \tag{17}$$

where ξ_1 and ξ_2 are the coordinate system in the reference element, and $\bar{\xi}_i$ is the coordinate of the ith grid node in the direction of ξ_1 ($\bar{\xi}_j$ is the coordinate of the jth grid node in the direction of ξ_2). The basis function, $h_{ij}(\xi_1,\xi_2)$, is equal to one on the corresponding grid node, $\xi_1 = \bar{\xi}_i$ and $\xi_2 = \bar{\xi}_j$, and zero on the other grid nodes. Clearly, an arbitrary function f in the reference element can be uniquely approximated as a summation of these basis functions over all the grid nodes:

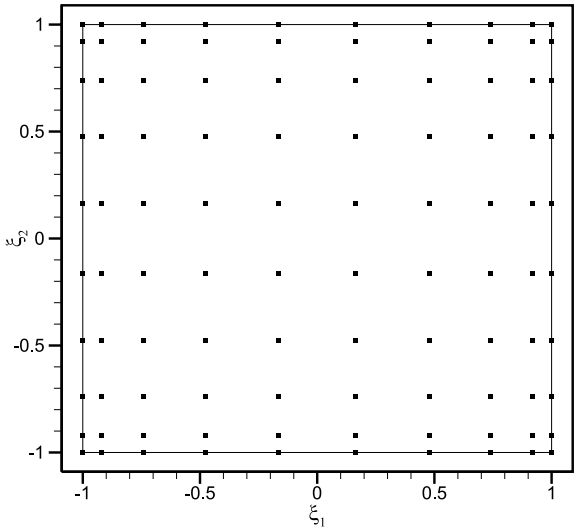

Fig. 1. GLL grid nodes on the reference element used to express the basis for a nineth-order polynomial space.

$$f(\xi_1,\xi_2) \approx f_h(\xi_1,\xi_2) = \sum_{j=0}^{N}\sum_{i=0}^{N} f_{ij} h_{ij}(\xi_1,\xi_2), \tag{18}$$

where $f_h(\xi_1,\xi_2)$ is called the discretized function.

3.2. Numerical integration

The integrands appearing in the SEM integrals involve higher order polynomials. To evaluate these integrals quadrature rules are more practical. GLL quadrature points, shown in Fig. 1 for a reference element, are used to numerically evaluate the integrals in the reference element. The advantage of using the same points both for defining bases functions and for the numerical quadrature is the convenient evaluation of the Lagrange interpolants at the grid points:

$$\int_{-1}^{1}\int_{-1}^{1} f(\xi_1,\xi_2)\mathrm{d}\xi_1\mathrm{d}\xi_2 \approx \sum_{j=0}^{N}\sum_{k=0}^{N} f(\bar{\xi}_j,\bar{\xi}_k)\omega_j\omega_k, \tag{19}$$

where $\bar{\xi}_j$'s are the GGL quadrature nodes, and ω_j's are the weights associated with the quadrature nodes. The weights are given by

$$\omega_j = \frac{2}{N(N+1)}\frac{1}{P_N^2(x)}, \tag{20}$$

where $P_N(x)$ is the Legendre polynomial of degree N introduced earlier. Numerical integration based on GLL quadrature (19) gives the exact value of the integral provided that the function f is a polynomial of order at most $2N-1$ in each spatial direction. This is the case when numerically integrating

$$\int_{\Omega_{\mathrm{ref.}}} (\nabla h_{ij}\cdot\nabla h_{mn})\mathrm{d}\xi_1\mathrm{d}\xi_2, \tag{21}$$

on the reference element, but when calculating the mass matrix by evaluating

$$\int_{\Omega_{\mathrm{ref.}}} (h_{ij}h_{mn})\mathrm{d}\xi_1\mathrm{d}\xi_2, \tag{22}$$

an error is made because $(h_{ij}h_{mn})$ is of order $2N$, nevertheless the accuracy of the scheme is maintained [21]. Finally, the numerically calculated mass matrix is a diagonal matrix which is a direct consequence of the fact that the Lagrangian interpolants and the quadrature are both based on the GLL grid nodes.

The spatial discretization of a boundary value problem leads to a system of linear algebraic equations. The assembly of the resulting complex system of equations is described in the next section.

3.3. Resulting matrices

Since problems addressed can be complex problems, both the real part and the imaginary part of the solution must be solved. The discretization of the problem leads to a system of linear algebraic equations:

$$A\varphi = F. \tag{23}$$

Here A, φ and F have complex values:

$$(A_{\mathrm{R}} + \mathrm{i}A_{\mathrm{I}})\times(\varphi_{\mathrm{R}} + \mathrm{i}\varphi_{\mathrm{I}}) = F_{\mathrm{R}} + \mathrm{i}F_{\mathrm{I}}. \tag{24}$$

Therefore we have a block system of equations:

$$A_R\varphi_R - A_I\varphi_I = F_R,$$
$$A_I\varphi_R + A_R\varphi_I = F_I. \tag{25}$$

This means that the system to be solved is the following block system

$$\begin{bmatrix} A_R & -A_I \\ A_I & A_R \end{bmatrix}\begin{bmatrix} \varphi_R \\ \varphi_I \end{bmatrix} = \begin{bmatrix} F_R \\ F_I \end{bmatrix} \tag{26}$$

which can also be written as a symmetric system:

$$\begin{bmatrix} A_R & A_I \\ A_I & -A_R \end{bmatrix}\begin{bmatrix} \varphi_R \\ -\varphi_I \end{bmatrix} = \begin{bmatrix} F_R \\ F_I \end{bmatrix}. \tag{27}$$

This linear system is sparse, symmetric, indefinite and relatively ill-conditioned. Preconditioning of this system is required to efficiently solve the system iteratively. This important aspect of the solution process is not studied here as only commonly available preconditioners are used. Other preconditioners based on finite element discretization [22] or additive Schwarz method [23] will be studied in future work. Therefore, the system (27) is solved using a conjugate-gradient iterative solver with ILU, SSOR, or Jacobi preconditioners [24], depending on the problem.

In the next section this method is applied to some sample problems.

4. Numerical results

This section reports the results of three sample problems solved with the spectral element method. Problems with different boundary conditions are chosen to validate the code. These problems also have analytical solutions. Consequently, the comparison of the numerical results and the analytical solution is discussed. In the next section, the spectral element method is also compared with a second-order finite element method to investigate its efficiency.

4.1. Green's function problem

The first problem is called Green's function on a rectangular domain. In this problem the performance and the accuracy of the method for a problem with a point source function and homogeneous Dirichlet boundary conditions are examined.

The problem of finding Green's function φ within a rectangular domain Ω with homogeneous Dirichlet boundary conditions is described by

$$\nabla^2\varphi(x,y) + k^2\varphi(x,y) = -\delta(x-x_0, y-y_0) \quad \text{in } \Omega, \tag{28}$$

$$\varphi(0,y) = \varphi(L_x,y) = \varphi(x,0) = \varphi(x,L_y) = 0. \tag{29}$$

The problem is solved for $L_x = L_y = 1$ and $x_0 = y_0 = 0.8$. Fig. 2 shows the result for $k = 10\pi/3$ using the spectral element method with $N = 1$ on a mesh 40×40. This first-order approximation is mainly used to plot the solution. It shows standing waves in the domain created by a point source.

The analytical solution of this problem is a series of eigenfunctions ψ_{ij} with amplitudes α_{ij} which are dependent on the wave number k:

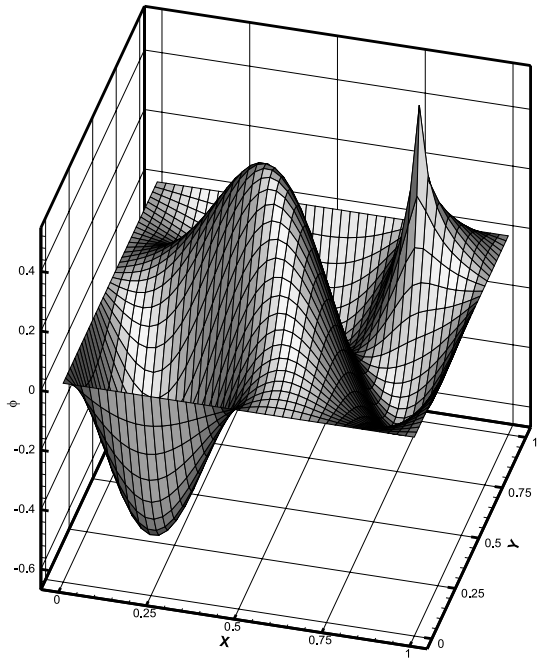

Fig. 2. Solution to the Green's function problem, $k = 10\pi/3$, mesh 40×40.

$$\varphi(x,y) = \sum_{i=1}^{\infty} \sum_{j=1}^{\infty} \alpha_{ij} \psi_{ij}(x,y), \tag{30}$$

where

$$\psi_{ij}(x,y) = \sin\left(\mathrm{i}\pi \frac{x}{L_x}\right) \sin\left(\mathrm{j}\pi \frac{y}{L_y}\right), \tag{31}$$

$$\alpha_{ij} = \frac{-4\psi_{ij}(x_0,y_0)}{L_x L_y (k^2 - (\mathrm{i}\pi/L_x)^2 - (\mathrm{j}\pi/L_y)^2)}. \tag{32}$$

Note that the solution does not have an imaginary part, therefore only standing waves are present in the domain.

In Fig. 3, the numerical solution for a higher wave number, $k = 40\pi/3$, is compared with the exact solution, which shows a very good agreement. Here the mesh is 10×10 and the order is five, $N = 5$. We now discuss the behavior of the solution with respect to the wave number. In Fig. 4(a), the same mesh and the same order of approximation is applied for an even higher wave number, $k = 70\pi/3$ leading to a poor result. To illustrate the pollution effect, the number of elements per wavelength is kept constant by dividing both the wave number and the number of elements in each direction by two and a slice of the solution is presented in Fig. 4(b). As noticed, a better agreement between the numerical solution and the exact solution is observed and reported in Table 1. This shows that the solution accuracy is highly sensitive to the wave number and not only to the number of elements per wavelength. Table 2 reports a comparison between the spectral element method with the second-order Galerkin finite element method. In this example, again the number of elements per wavelength is kept constant. The results show that while the error of the second-

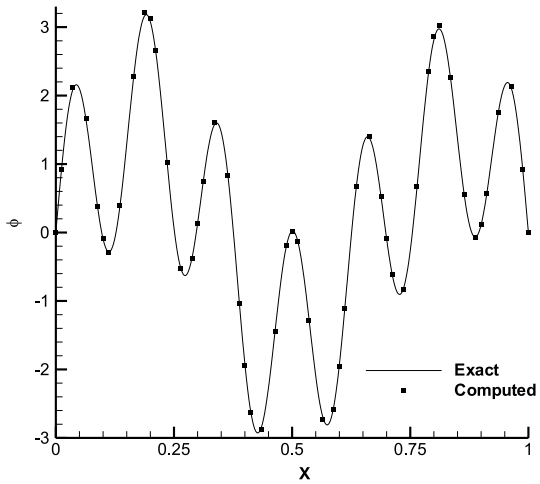

Fig. 3. Solution to the Green's function problem, $y = 0.2$, $k = 40\pi/3$, mesh 10×10, order five.

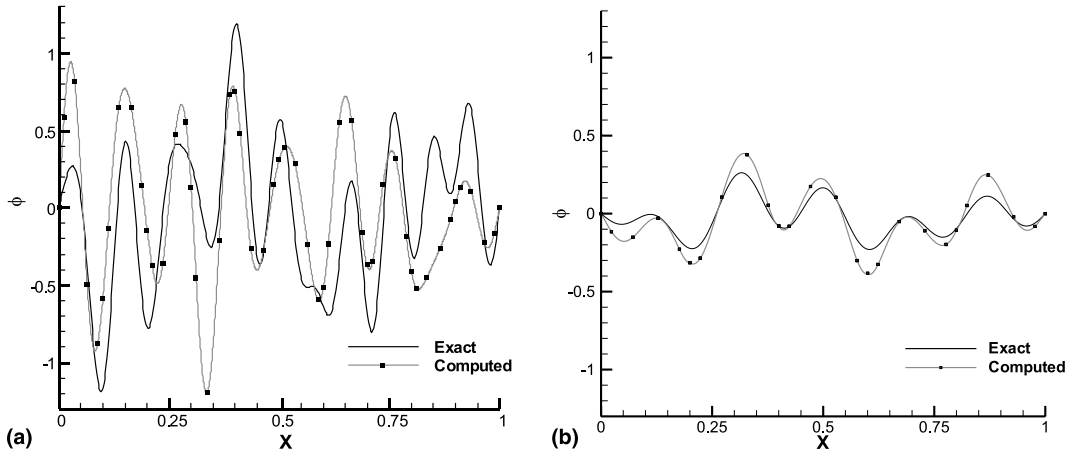

Fig. 4. Solution to the Green's function problem, (a) $y = 0.2$, $k = 70\pi/3$, mesh 10×10, order five, (b) $y = 0.2$, $k = 35\pi/3$, mesh 5×5, order five.

Table 1
Comparison of the L_2 error for two different wave numbers

k	Mesh	N	L_2 norm of the error
$70\pi/3$	10×10	5	3.86e−1
$35\pi/3$	5×5	5	8.58e−2

Table 2
Comparison of the spectral element and the second-order Galerkin finite element

k	Mesh	N	L_2 norm of the error	k	Mesh	N	L_2 norm of the error
$18\pi/3$	30×30	2	4.99e−3	$36\pi/3$	60×60	2	1.06e−2
$48\pi/3$	5×5	9	5.29e−3	$96\pi/3$	10×10	9	5.96e−3

order finite element increases by increasing the wave number, the error of the spectral element method remains almost the same. In other words, the pollution effect for high order spectral element is less dominant compare to the finite element method.

4.2. Closed wave-guide

A standing plane wave within a closed rectangular wave-guide is presented. This problem deals with non-homogeneous Dirichlet boundary conditions at one end, homogeneous Dirichlet boundary conditions at the other end and homogeneous Neumann boundary conditions on the two sides of the wave-guide. The equation describing this problem is:

$$\nabla^2\varphi(x,y) + k^2\varphi(x,y) = 0 \quad \text{in } \Omega, \tag{33}$$

$$\varphi(0,y) = g_0, \quad \varphi(L_x,y) = 0, \quad \frac{\partial\varphi}{\partial y}(x,0) = \frac{\partial\varphi}{\partial y}(x,L_y) = 0, \tag{34}$$

where Ω is the computational domain of size L_x and L_y. The standing plane wave can be calculated analytically by

$$\varphi(x,y) = g_0\frac{\sin(k(L_x - x))}{\sin(kL_x)}. \tag{35}$$

The problem is solved for wave number $k = 8\pi/3$ and $L_x = L_y = 1$. Fig. 5 shows the standing wave on the wave-guide, using a first-order approximation on a 30×30 mesh.

To study the accuracy of the spectral element method, the number of grid points is kept fixed while the order is increased and the number of elements is decreased. Fig. 6 presents the exact solution and different computed solutions. It is clear that as the order of the approximation increases the solution is more accurate.

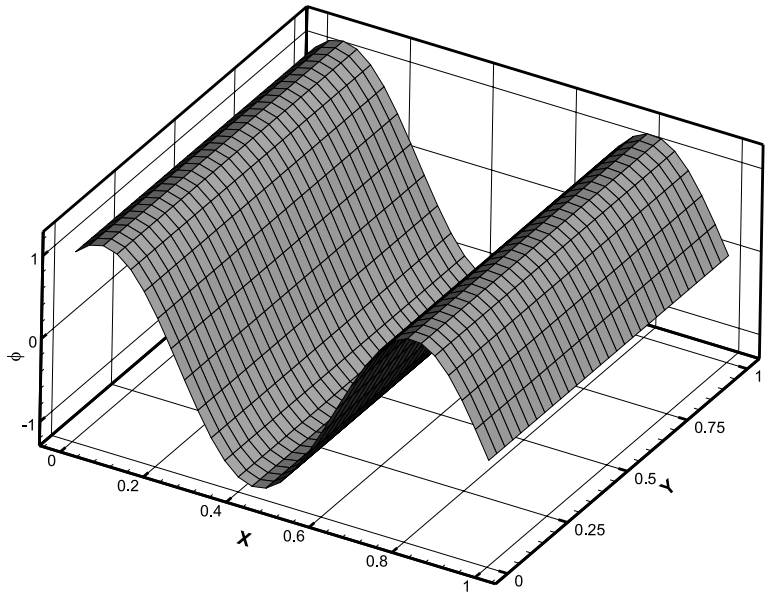

Fig. 5. Standing plane wave in a rectangular wave-guide, $k = 8\pi/3$, mesh 30×30.

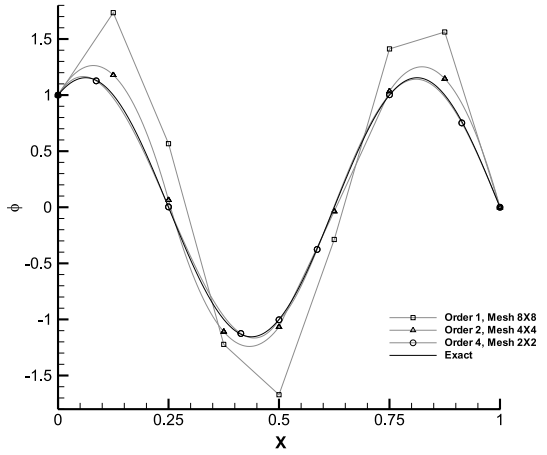

Fig. 6. Standing plane wave in a rectangular wave-guide, $k = 8\pi/3$, $y = 0.5$.

4.3. Semi-infinite wave-guide

Homogeneous and non-homogeneous Dirichlet and Neumann boundary conditions have been examined on simple geometries. In the last problem the PML method for treating an open boundary in a semi-infinite wave-guide is examined. The physical domain Ω is a rectangular wave-guide closed on two sides and at one end. The other end of the wave-guide is extended to infinity. The Helmholtz's equation has no source term hence the equation can be written as

$$\nabla^2\varphi(x,y) + k^2\varphi(x,y) = 0 \quad \text{in } \Omega. \tag{36}$$

The boundary conditions are

$$\varphi(0,y) = c_1\sin(l_1 y) + c_2\sin(l_2 y), \quad 0 < y < \pi, \tag{37}$$

$$\varphi(x,0) = \varphi(x,1) = 0, \quad 0 < x < \infty. \tag{38}$$

The exact solution to this problem is

$$\varphi(x,y) = c_1\exp\left(-\mathrm{i}\sqrt{k^2 - l_1^2}x\right)\sin(l_1 y) + c_2\exp\left(-\sqrt{l_2^2 - k^2}x\right)\sin(l_2 y). \tag{39}$$

It should be noted that the complex solution to $\varphi(x,y)$ in this problem is associated with traveling waves as opposed to standing waves as in the previous problems.

The solution to this problem for $0 < x \leqslant 5\pi$ is sought. The domain is therefore truncated at $x = 5\pi$. To prevent the reflection of the outgoing waves back into the domain, an artificial absorbing layer is added after the truncated boundary, $5\pi < x \leqslant 6\pi$. Due to the PML method, the variational weak form (10) instead of the original variational formulation of the problem (6) is solved. Here the parameters of the PML method are

$$\sigma_y(y) = 0, \sigma_x(x) = 0, \quad 0 < x < 5\pi, \tag{40}$$

$$\sigma_x(x) = 40\left(\frac{x - 5\pi}{\pi}\right)^2, \quad 5\pi \leqslant x \leqslant 6\pi. \tag{41}$$

The problem is solved for $k = 1.25$, $l_1 = 1$, $l_2 = 2$, $c_1 = 2$ and $c_2 = 1$, using a 6×1 mesh with eighth-order approximation. The real and imaginary results on the computation domain are presented in Figs. 7 and 8.

In Figs. 9 and 10, numerical results are compared with analytical solutions for both real and imaginary solutions. From these figures, note that the absorbing layer absorbs the waves and the amplitude of the waves goes to zero in the absorbing layer.

5. Efficiency investigation

To investigate the efficiency of the spectral element method, its spatial L_2 norm convergence is compared with second-order finite element method ($N = 2$), which has been considered as a classic finite element method. Furthermore, the computational cost, i.e., the total CPU time, of the spectral element method is compared with the second-order finite element method.

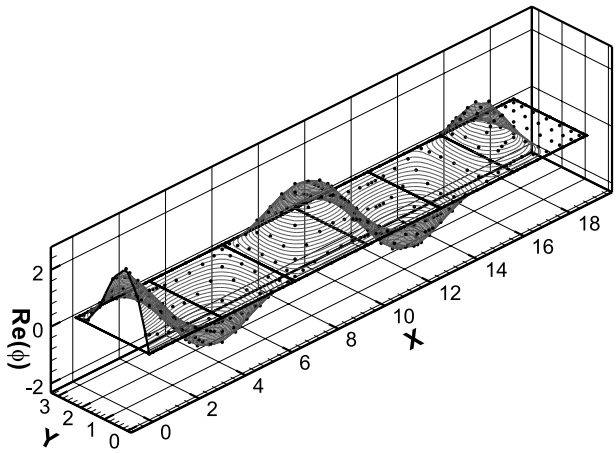

Fig. 7. Semi-infinite wave-guide solution, real part.

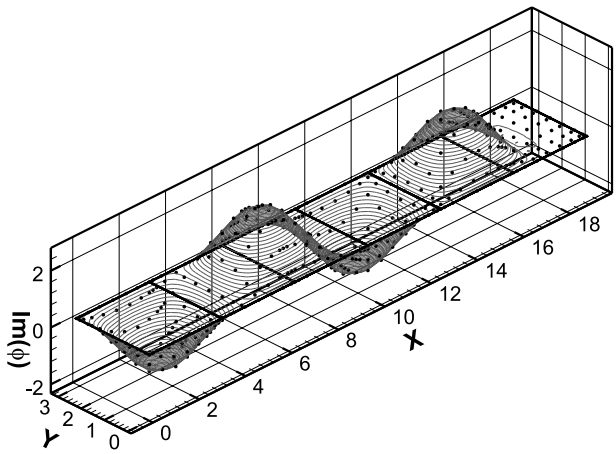

Fig. 8. Semi-infinite wave-guide solution, imaginary part.

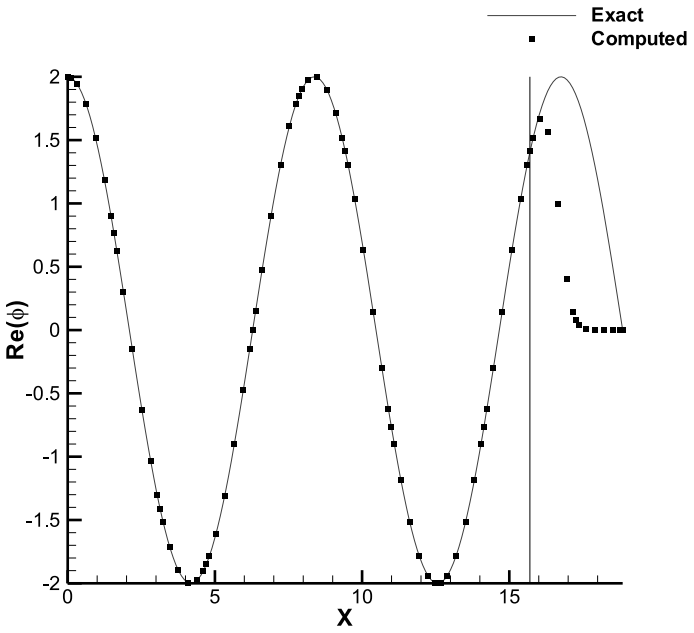

Fig. 9. Semi-infinite wave-guide solution, real part, $y = 0.5\pi$.

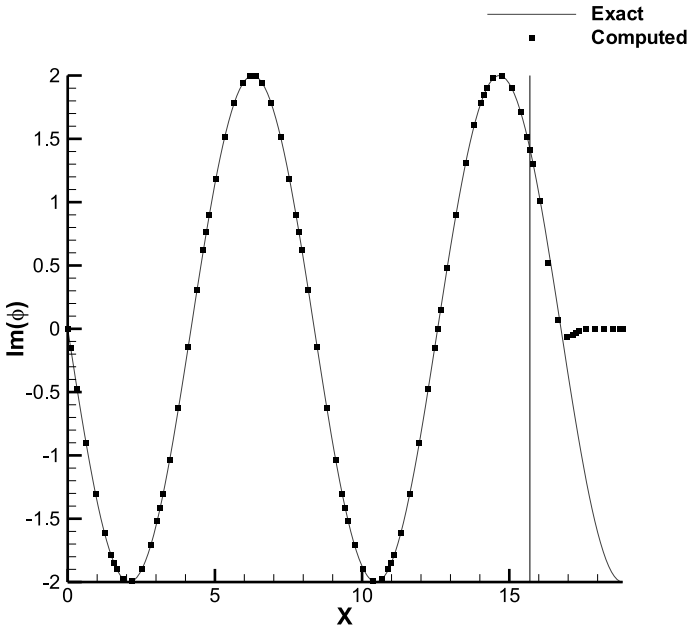

Fig. 10. Semi-infinite wave-guide solution, imaginary part, $y = 0.5\pi$.

The L_2 norm of the error is defined as

$$\|e\|_2 \equiv \sqrt{\int_\Omega (\varphi_{\text{computed}} - \varphi_{\text{exact}})^2 \mathrm{d}x\,\mathrm{d}y}. \tag{42}$$

In Fig. 11, the error in the L_2 norm for Green's function problem is plotted against the degrees of freedom, i.e., number of the grid points. The first curve shows the spatial convergence due to increasing the number of elements and keeping the order, N, constant, h-extension. In the second curve, the number of the elements is kept constant and the order, N, is increased to achieve higher accuracy, p-extension. The curves are presented in log–log and semi-log scales. Figs. 12 and 13 show the same comparison for the closed wave-guide and for the semi-infinite wave-guide. These comparisons clearly show the advantage of the spectral element methods in terms of exponential convergence rate as dictated by theory for smooth solutions.

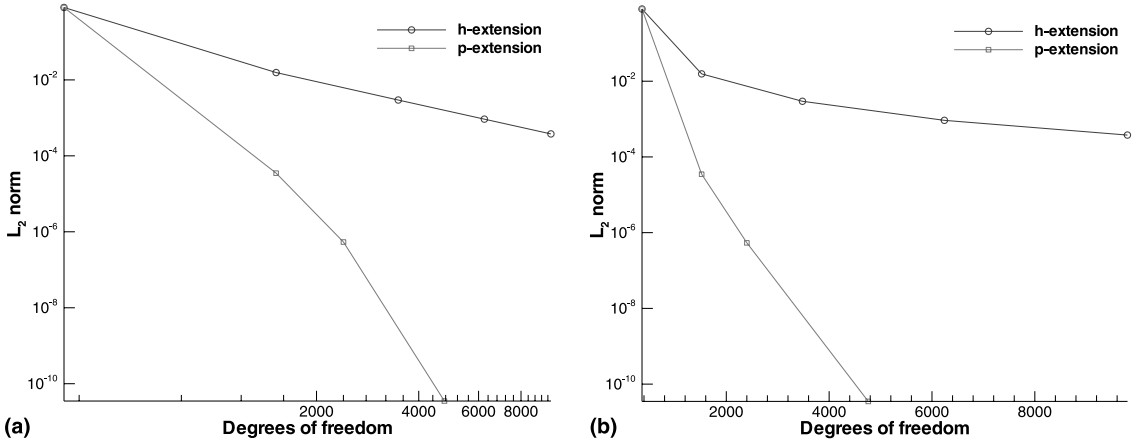

Fig. 11. Spatial convergence for Green's function problem, $k = 20\pi/3$: (a) log–log scale, (b) semi-log scale.

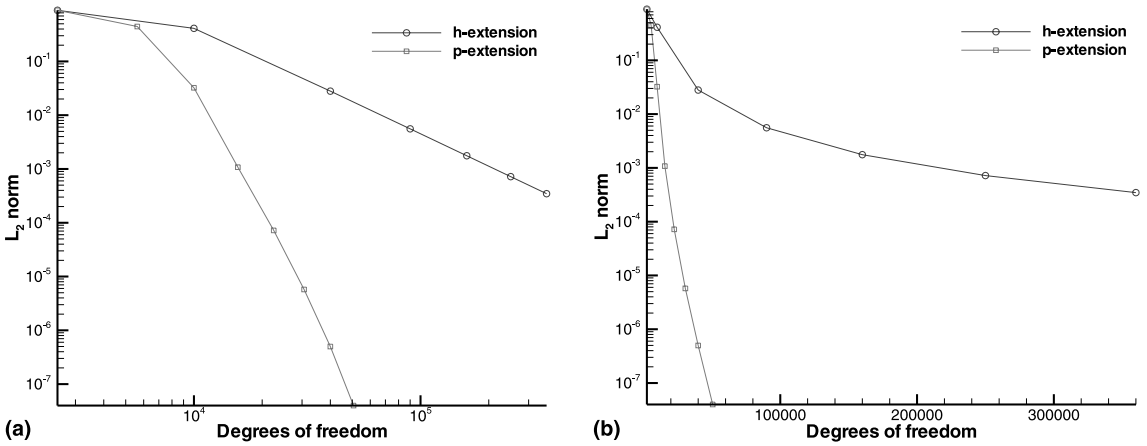

Fig. 12. Spatial convergence for standing plane wave in a closed wave-guide, $k = 100\pi/3$: (a) log–log scale, (b) semi-log scale.

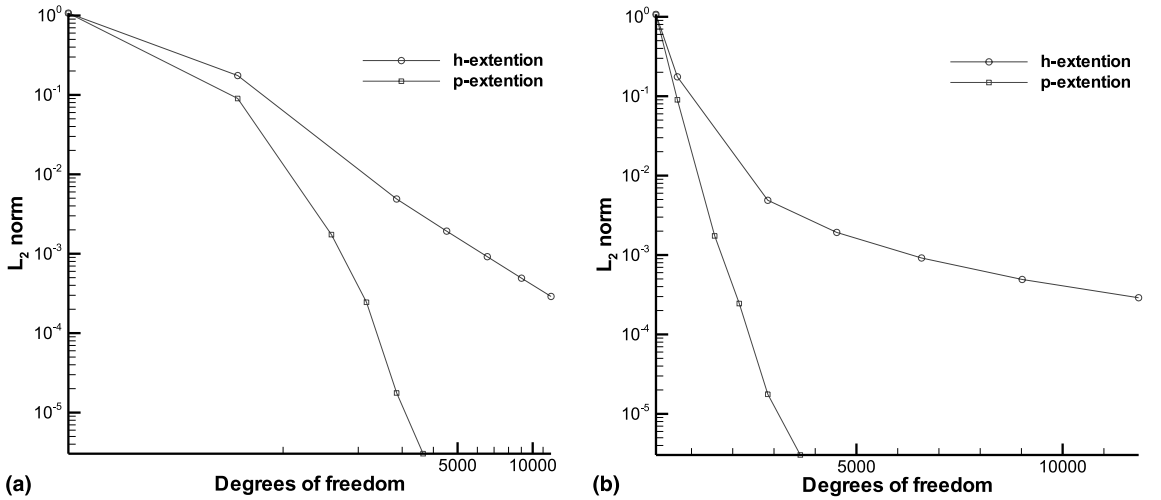

Fig. 13. Spatial convergence for semi-infinite wave-guide, $k = 1.25$: (a) log–log scale, (b) semi-log scale.

Clearly, the number of degrees of freedom is not the only parameter determining the numerical cost of solving a problem when iterative solvers are used. The sparseness and condition number of the matrix are other influential parameters. Higher order elements lead to less sparse and therefore harder to solve matrices, so it is important to examine not only the size of the matrix but also its properties. Obviously, preconditioners play a huge role for the computation cost.

In this work, commonly available preconditioners are used with the conjugate-gradient iterative solver. The iterative solver and the preconditioners are from LASPack library [24]. For Green's function the SSOR preconditioner is used and for the closed wave guide the Jacobi preconditioner is used. The system associated with the semi-infinite wave-guide is preconditioned with an ILU(0) preconditioner.

In LASPack the iterative solver stops if the residual satisfies the condition:

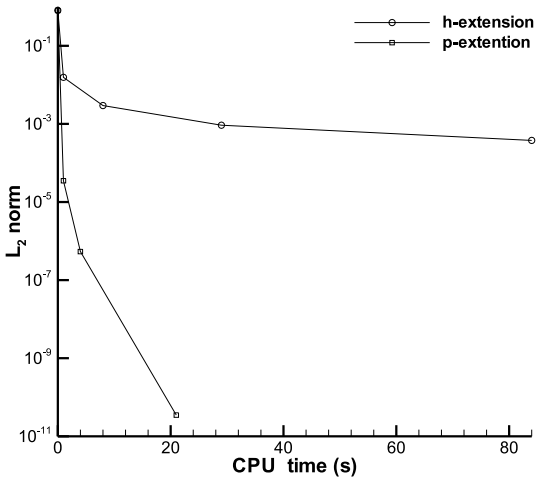

Fig. 14. CPU time for Green's function problem.

$$\|r\|_2 = \|F - A\varphi\|_2 \leqslant \varepsilon \|F\|_2, \tag{43}$$

where ε is the accuracy defined by LASPack termination control, and is set to 10^{-8}.

Furthermore, the assembling cost plays an important role in the computational cost, depending on the problem. So in order to show the efficiency of the spectral element method in terms of the computational cost, the comparison of the CPU time is necessary. In this regard, in Figs. 14–16 the total computational cost is compared for the two methods.

These results clearly show that not only the spectral element method leads to smaller system to be solved, but also the total CPU time for the spectral element method is much less than the total CPU time for the finite element method for same accuracy. Furthermore, Fig. 16 shows that the spectral element method is more robust for PML in comparison to the finite element method.

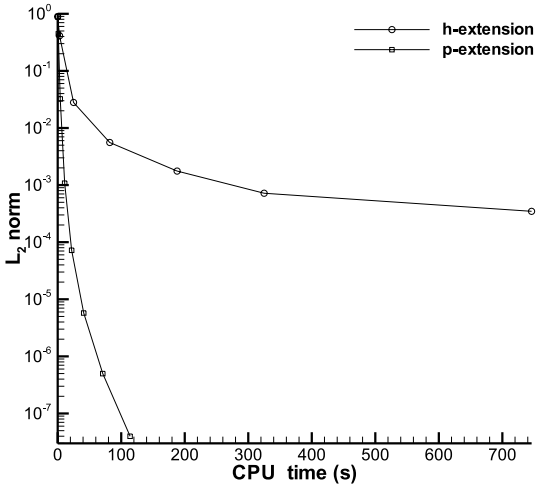

Fig. 15. CPU time for standing plane wave in a closed wave-guide.

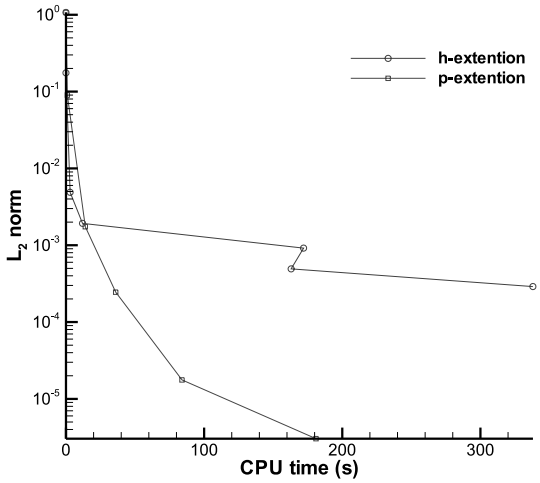

Fig. 16. CPU time for semi-infinite wave-guide.

Table 3
Preconditioned conjugate gradient iterations for Green's function problem, $\varepsilon = 10^{-8},\ k = 20\pi/3$

h-Extension		p-Extension	
Degrees of freedom	Number of iterations	Degrees of freedom	Number of iterations
361	86	361	86
1521	111	1521	126
3481	154	2401	153
6241	198	4761	216
9801	245		

Table 4
Preconditioned conjugate gradient iterations for a closed wave-guide, $\varepsilon = 10^{-8},\ k = 100\pi/3$

h-Extension		p-Extension	
Degrees of freedom	Number of iterations	Degrees of freedom	Number of iterations
2499	137	2499	137
9999	167	5624	135
39,999	330	9999	201
89,999	493	15,624	268
159,999	655	22,499	341
249,999	818	30,624	471
359,999	1501	39,999	538
		50,624	574

Table 5
Preconditioned conjugate gradient iterations for semi-infinite wave-guide, $\varepsilon = 10^{-8},\ k = 1.25$

h-Extension		p-Extension	
Degrees of freedom	Number of iterations	Degrees of freedom	Number of iterations
138	33	138	33
658	67	658	80
2850	482	1562	147
4522	1308	2158	175
6578	14,041	2850	404
9018	9241	3638	597
11,842	14,737		

Finally, the number of iterations of the solver, preconditioned conjugate gradient, are reported in Tables 3–5 for the three problems addressed. Clearly, there is a need to develop appropriate preconditioners for the linear systems arising from Helmholtz problem.

6. Conclusion

It is known that Galerkin finite element solution to Helmholtz's equation is computationally expensive, and needs large computation resources, for high wave numbers, due to the pollution effect. The results of this work show that the spectral element method, as an alternative to finite element methods, is more efficient for solving two-dimensional Helmholtz's equation in terms of both memory and computational cost,

i.e., it offers exponential convergence and less pollution. It also offers the same advantages of finite element methods. In other words, it has the potential for addressing problems in geometrically complex and non-homogeneous domains, which is usually the case for the real acoustic problems such as acoustic field in a silencer. Nevertheless more work is required to develop appropriate preconditioners for the linear system arising from the discretization of the weak form of Helmholtz's equation. This paper also shows that the PML boundary conditions are applicable for the spectral element method and preserve the exponential convergence rate. Therefore, this method can also address unbounded problems.

Acknowledgements

This work was supported by Materials and Manufacturing Ontario (MMO) and by the National Science and Engineering Research Council of Canada (NSERC).

References

[1] R. Tezaur, A. Macedo, C. Farhat, R. Djellouli, Three-dimensional finite element calculations in acoustic scattering using arbitrarily shaped convex artificial boundaries, Int. J. Numer. Meth. Eng. 53 (6) (2002) 1461–1476.
[2] R. Ramakrishnan, W.R. Watson, Design curves for rectangular splitter silencers, Appl. Acoust. J. 35 (1992) 1–24.
[3] G.D. Manolis, R.P. Shaw, Harmonic wave propagation through viscoelastic heterogeneous media exhibiting mild stochasticity – I. Fundamental solutions, Soil Dyn. Earthq. Eng. 15 (2) (1996) 119–127.
[4] R.P. Ratowsky, J.A. Fleck Jr., M.D. Feit, Helmholtz beam propagation in rib waveguides and couplers by iterative lanczos reduction, Opt. Soc. Am. A 9 (1992) 256.
[5] M.C. Junger, D. Feit, Sound, structures and their interaction, second ed., MIT Press, Cambridge MA, 1986.
[6] K. Kashiyama, M. Sakuraba, Adaptive boundary-type finite element method for wave diffraction-reflection in harbours, Comput. Meth. Appl. Mech. Eng. 112 (1994) 185–197.
[7] J.R. Stewart, T.J.R. Hughes, Explicit residual-based a posteriori error estimation for finite element discretizations of the Helmholtz equation: computation of the constant and new measures of error estimator quality, Comput. Meth. Appl. Mech. Eng. 131 (3–4) (1996) 335–363.
[8] R.P. Shaw, Integral equation methods in acoustics, in: C.A. Brebbia (Ed.), Boundary Elements X, vol. 4, Springer, Berlin, 1988, pp. 221–244.
[9] L.G. Copely, Fundamental results concerning integral representations in acoustic radiation, J. Acoust. Soc. Am. 44 (1) (1968) 28–32.
[10] I. Harari, T.J.R. Hughes, Finite element methods for the Helmholtz equation in an exterior domain: model problems, Comput. Meth. Appl. Mech. Eng. 87 (1) (1991) 59–96.
[11] D. Givoli, I. Harari (Eds.), Exterior problems of wave propagations (special issue), Comput. Meth. Appl. Mech. Eng. 164(1–2) (1998) 1–2.
[12] I. Harari, T.J.R. Hughes, A cost comparison of boundary element and finite element methods for problems of time-harmonic acoustics, Comput. Meth. Appl. Mech. Eng. 97 (1992) 77–102.
[13] I. Babuška, F. Ihlenburg, E.T. Paik, S.A. Sauter, A generalized finite element method for solving the Helmholtz equation in two dimensions with minimal pollution, Comput. Meth. Appl. Mech. Eng. 128 (1995) 325–359.
[14] L.L. Thompson, P.M. Pinsky, A Galerkin least-squares finite element method for the two-dimensional Helmholtz equation, Int. J. Numer. Meth. Eng. 38 (3) (1995) 371–397.
[15] F. Ihlenburg, I. Babuška, Finite element solution of the Helmholtz equation with high wave number. Part I: the h-version of the FEM, Comput. Math. Appl. 30 (9) (1995) 9–37.
[16] I. Harari, T.J.R. Hughes, Galerkin/least-squares finite element methods for the reduced wave equation with nonreflecting boundary conditions in unbounded domains, Comput. Meth. Appl. Mech. 98 (3) (1992) 411–454.
[17] I. Harari, C.L. Nogueria, Reducing dispersion of linear triangular elements for the Helmholtz equation, J. Eng. Mech. 128 (3) (2002) 351–358.
[18] Y. Maday, A.T. Patera, Spectral element methods for incompressible Navier–Stokes equations, in: A.K. Noor, J.T. Oden (Eds.), State-of-the-Art Surveys on Computational Mechanics, ASME, New York, 1989, pp. 71–143.
[19] P.F. Fischer, An overlapping Schwarz method for spectral element solution of the incompressible Navier–Stokes equations, J. Comput. Phys. 133 (1) (1997) 84–101.

[20] I. Harari, M. Slavutin, E. Turkel, Analytical and numerical studies of a finite element PML for the Helmholtz equation, J. Comput. Acoust. 8 (1) (2000) 121–137.
[21] G.C. Cohen, Higher-order numerical methods for transient wave equations, Springer, Berlin, 2002.
[22] L. Pavarino, E. Zampieri, Preconditioners for spectral discretizations of Helmholtz's equation with Sommerfeld boundary conditions, Comput. Methods Appl. Mech. Engrg. 190 (2001) 5341–5356.
[23] X.-C. Cai, O.B. Widlund, Domain decomposition algorithms for indefinite elliptic problems, SIAM J. Sci. Stat. Comp. 13 (1992) 243–258.
[24] T. Skalicky, LASPack reference manual, version 1.12.3, Dresden University of Technology, Institute for Fluid Mechanics, Dresden, Germany (1996).